Prediction of Formability in Perovskite-Type Oxides

A. Kumar[1,2], A.S. Verma[*,1,3] and S.R. Bhardwaj[1]

[1]*Department of Physics, B. S. A. College, Mathura, 281004, India*

[2]*Department of Physics, K. R. (P.G.) College, Mathura, 281001, India*

[3]*Department of physics, Sanjay Institute of Engineering and Management, Mathura, 281406, India*

Abstract: Prediction criterions for the formabilities of perovskite-type oxides are obtained by using the empirical structure map methods constructed by two parameters octahedral factor (r_B/r_O) and tolerance factor, on this structure map, simple point representing systems of forming and non forming are distributed in distinctively different regions. In this paper we found that the octahedral factor, is as important as the tolerance factor with regards to the formability of perovskite-type oxides. We have applied the proposed model to 173 ABO_3 perovskites and it can be used to search for new perovskite-type oxides by screening all possible elemental combinations.

INTRODUCTION

A large number of perovskite-type oxides have been studied because of their interesting properties, including superconductivity, insulator–metal transition, ionic conduction characteristics, dielectric properties and ferroelasticity [1-3]. Additionally, they have received great attention as high temperature proton conductors with the possibility of applications in fuel cells or hydrogen sensors. Perovskite is one of the most frequently encountered structures in solid-state physics, and it accommodates most of the metallic ions in the periodic table with a significant number of different anions. During the last few years, many experimental and theoretical investigations were devoted to the study of perovskite solids: typically ABX_3 (A: large cation with different valence, B: transition metal and X: oxides and halides). These solids are currently gaining considerable importance in the field of electrical ceramics, refractories, geophysics, astrophysics, particle accelerators, fission, fusion reactors, heterogeneous catalysis etc [4-7]. In perovskite structures, which is shown in Fig. (**1a**), B cations are coordinates by six X anions, while A cations present coordination number 12 (also coordinated by X anions). The X anions have coordination number 2, being coordinated by two B cations, since the distance A—X is about 40% larger than the B—X bond distance. The cubic perovskite is called the ideal perovskite, which is the subject of this study. This class of materials has great potential for a variety of device applications due to their simple crystal structures and unique ferroelectric and dielectric properties [8-15]. As one of the most abundant and widely investigated minerals, perovskites solids are widely studied as the candidate materials of substrate materials. For example, cubic perovskites has recently gained widespread usage as a substrate or buffer material for the heteroepitaxial growth of high temperature superconductors and other oxide thin films [16]. A perovskite-type crystal (orthorhombic distorted perovskites), $NdGaO_3$, was reported as a succeeded candidate for the GaN substrate [17]; $(La,Sr)(Al,Ta)O_3$ (LSAT) [18] and $(RE,Sr)(Al,Ta)O_3$ (RE, rare earth elements) [19], the mixed perovskite-type oxide, have very good characteristics to be a substrate since it has a fairly small lattice mismatch with GaN. In general, the semiconductor, which has zinc blende structure, can grow on the substrate or buffer layers with cubic structure. The recent success of fabricating large GaAs MESFETs on Si substrates using an $SrTiO_3$ (cubic perovskites) as buffer layer increases the interest of investigating cubic perovskites [20].

Many researchers try to design and synthesize new cubic perovskites used as substrate materials. Obviously, if new cubic perovskites compounds and their lattice constants can be predicted, it is helpful to design new substrate or buffer materials with cubic perovskite structure. Recently, the authors [21], a proposed model of lattice constant in cubic perovskites ABX_3 was obtained by using average ionic radii (r_{av}), of ABX_3. So, it is of practical and emergent to find out regularities governing the formation of cubic perovskite-type oxides in order to seek for new buffer materials or substrates for compound semiconductor direct growth. We have investigated the regularities governing perovskites formation by using empirical structure map methods and a total 173 perovskite oxide systems. It is found that the octahedral factor (r_B/r_O) is as important as the tolerance factor (t), with regard to the formability of perovskites.

STRUCTURAL MAP METHOD

First, Mooser and Perason [22] applied a two-dimension graphic to study the stability of different compounds, the two factors they used were the difference of electronegativity between the cation and the anion and the average principle quantum number. They succeeded to discriminate the crystal structures of AB-type compounds, of AX_2-type halides, and the metallic or non-metallic ternary fluorides ABX. Similar methods were called the structural map technology, and more parameters were used to draw the graphic. Muller and Roy [23] proposed to plot ''structural map'', which took the ionic radius of A and B as coordinates to study the distribution of different structures for many ternary structural families. Furthermore, the schematic distribution map of different

*Address correspondence to this author at the Department of physics, Sanjay Institute of Engineering and Management, Mathura, 281406, India;
E-mail: dr.ajyphy@rediffmail.com

1874-1835/08 2008 Bentham Open

crystal structure for $A^{+1}B^{+5}X_3$, $A^{+2}B^{+4}X_3$ and $A^{+3}B^{+3}X_3$ systems separately, were given by the same method [23, 24]. However, the criterion for perovskite formability was not discussed, possibly due to the lack of accurate data of crystal structure of some ABX_3 compounds at that time. The ionic radius is the most important ionic parameter that dominates the crystal structure of ionic compound. In this study, the same method will be used to find the regularities governing cubic perovskites formability. Prediction criterions for the formability of perovskites are obtained by using these two parameters tolerance factor and octahedral factor.

The ideal cubic structure form may be seen as a network of BX_6 octahedra, where all the octahedra are corner sharing. The *A* ions occupy the cubo-octahedral holes in between the octahedra. Many derivatives of the ideal structure are found and the distortion of the structure from cubic is often considered to be determined by the relative sizes of the different ions of the compound. The much used tolerance factor (t) is defined as

$$t = r_A + r_X / \sqrt{2}\,(r_B + r_X) \quad (1)$$

where r_A, r_B and r_X are the ionic radii of A, B and X_3 respectively. t=1 corresponds to an ideal perovskite, while a $t<1$ indicates tilting or rotation of the BX_6 octahedra. A $t>1$ indicates preference for hexagonal perovskite structures, where the octahedra at least to some extent share faces. The face-sharing octahedra then form chains along the hexagonal *c* axis, bound to each other by *A*-X bonds. The face sharing octahedra give relatively short *B*-*B* distances, thus increasing the electrostatic repulsion between the *B*-site cations. Hexagonal stacking and face sharing is therefore introduced in stages with increasing size of the *A* cation. Alkaline-earth-metal manganese oxides show this importance of size well [25]. $CaMnO_3$ forms an orthorhombic derivative of the cubic structure with slightly tilted octahedra [26]. At high temperatures $SrMnO_3$ takes a cubic perovskite structure with corner-sharing octahedra only (Fig. **1a**) [27]. At low temperatures, on the other hand, $SrMnO_3$ forms a four-layer hexagonal structure (Fig. **1b**) with both face-sharing and corner-sharing octahedra corresponding to hexagonal and cubic stacking, respectively. $BaMnO_3$ forms a hexagonal structure with face sharing of octahedra only. The stabilization of the hexagonal structures at low temperatures has long been ascribed to the formation of metal-metal interactions across the shared face [28]. However, the Mn-Mn *d*-orbital overlap has recently been shown to be minimal [25, 29] Instead covalent interactions between manganese and oxygen atoms are indicated. Both the relative sizes of the cations and the covalency of the Mn-O bonds appear to be important for stabilizing the hexagonal structures of $SrMnO_3$ and $BaMnO_3$ at low temperatures [25, 29].

Tolerance factor (t) has been widely accepted as a criterion for the formation of the perovskite structure, many researchers have used it to discuss the cubic perovskites stability, and therefore, it is an important factor for the stability of cubic perovskites, so tolerance factor (t) constructs one axe of the structure map. Another important octahedron factor (r_B/r_O) [30] is as important as the tolerance factor to form cubic perovskites, so octahedron factor constructs another axe of the two-dimension structure map. Which are shown in Fig. (**5**).

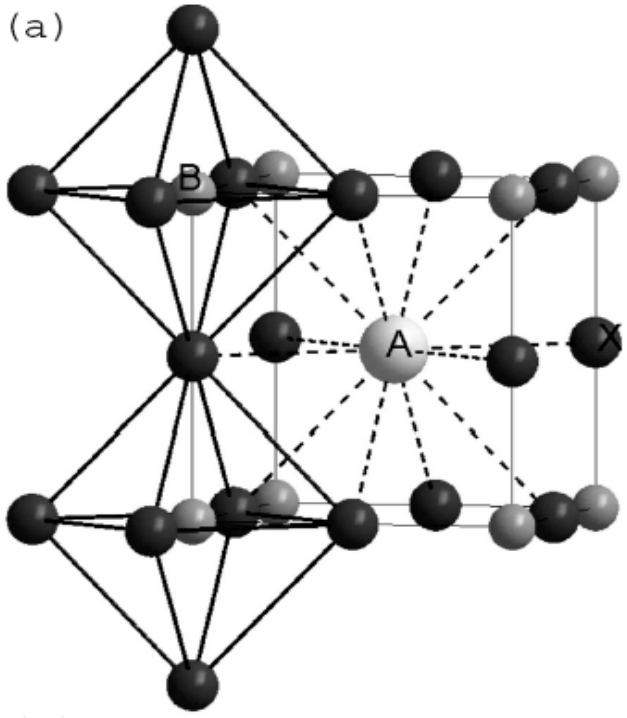

Fig. (1a). Ideal cubic perovskite structure.

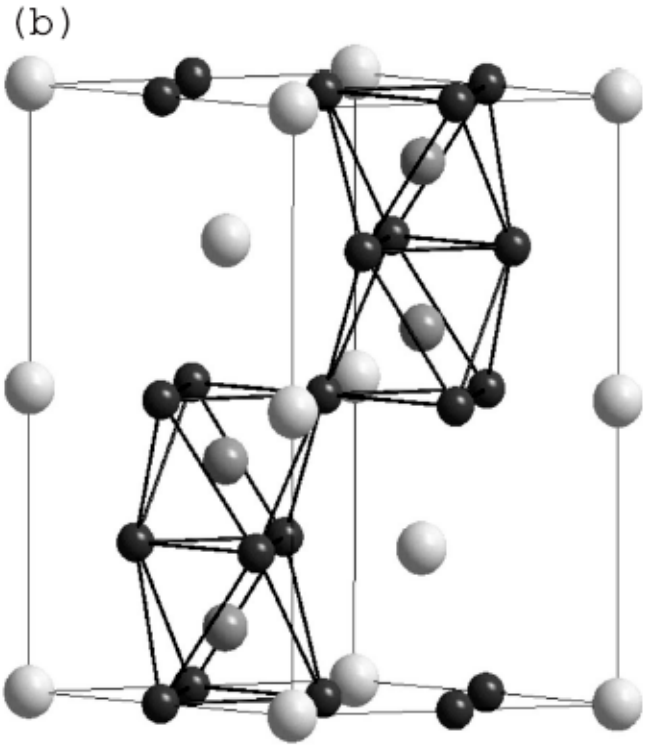

Fig. (1b). Four layer hexagonal perovskite structure.

RESULTS AND DISCUSSION

A total of 173 binary oxide systems are collected, as seen in Table **1**, of which, 29 systems (denote ''F'') are found to have cubic perovskite structure, 144 systems (denote ''NF'')

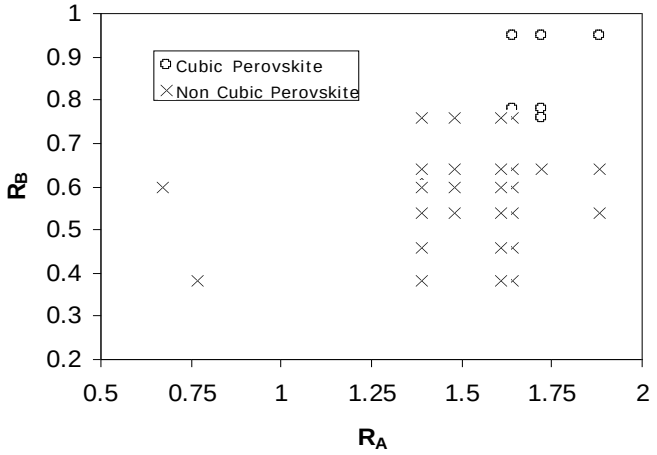

Fig. (2). Perovskite formability in ($A^{+}B^{5+}X_3$) oxide systems.

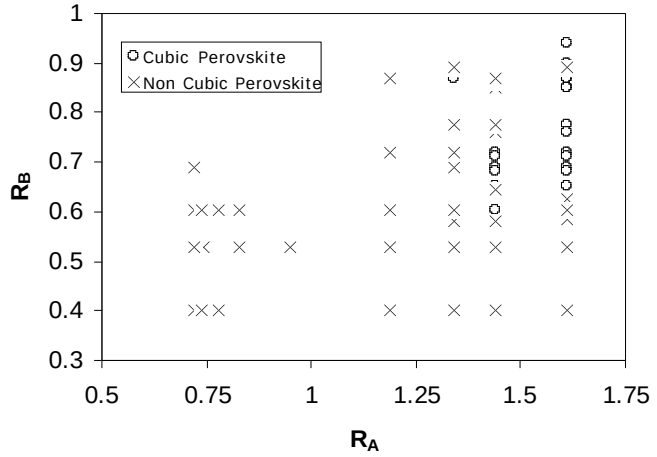

Fig. (3). Perovskite formability in ($A^{+2}B^{4+}X_3$) oxide systems.

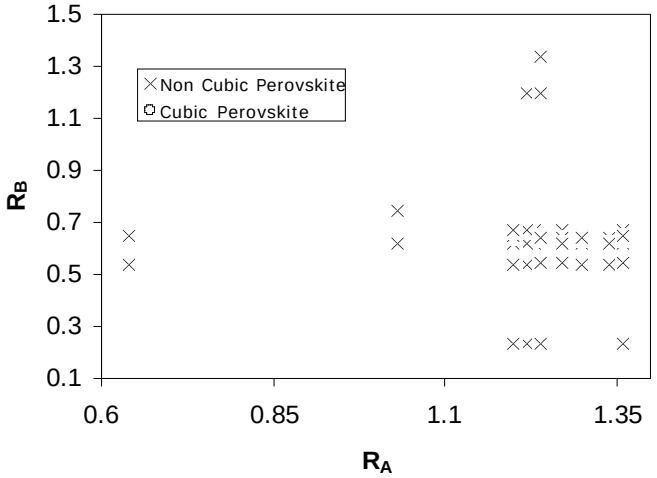

Fig. (4). Perovskite formability in ($A^{+3}B^{3+}X_3$) oxide systems.

can not form cubic perovskite structure. It is well known, a crystal structure can change with variation of temperature and/or pressure. Compounds with other structure can, therefore, transform into cubic perovskite structure, and vice verse at different temperature and/or pressure. So, the criterion for classifying a forming system is that a compound of cubic perovskites is stabilized at room temperature and one atmosphere pressure. 173 perovskite-type oxides systems with their formability, ionic radius of constituent ions A and B, tolerance factor and the octahedral factor (the ratio of radius of the small cation B over the radii of anion O) are listed in Table **1**. The ionic radius of r_A, r_B and r_X ($X = O^{-2}$ is 1.35 Å) are taken from [5, 8, 21, 33]. As shown in Figs. (**2**-**5**), all perovskites and non-perovskites are located in two different regions, and a clear border between two kinds of compounds is identified. In the Fig. (**5**), the criterion of perovskite formability is, then, expressed by the following equations:

$$r_B/r_O = 0.433 \quad (2)$$

$$t = 1.032 \quad (3)$$

$$t = 0.857 \quad (4)$$

$$r_B/r_O = -1.327 \{r_A + r_O / \sqrt{2} (r_B + r_O)\} + 1.781 \quad (5)$$

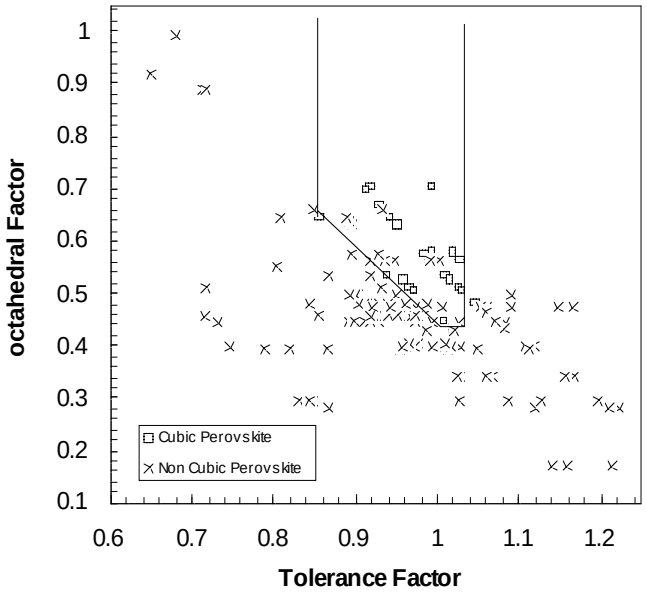

Fig. (5). Classification of cubic (ABO_3) perovskite oxides.

The tolerance factor is a widely used parameter in perovskites study, which takes all the ionic radii into consideration. And it is known that almost all perovskites have a t value ranging from 0.75 to 1.00. According to Goldschmidt's point, t values of cubic perovskites are in the range of 0.8–0.9. From Fig. (**5**), it is indicated that t values of cubic perovskites, except $BaMoO_3$, are in the range of 0.857–1.032, which is wider than Goldschmidt's range. However, t = 0.857–1.032 is a necessary but not a sufficient condition for the formation of the cubic perovskite structure. The 85 systems, the t values of which are in the range (0.857–1.032), can not form cubic perovskite structure.

Octahedral factor is introduced into prediction of cubic perovskites formation. In our structure map (Fig. **5**), the lowest limit of the octahedral factor for cubic perovskites formation is 0.433, and the highest r_B/r_O value of cubic perovskites is 0.704. It is well known that r_B/r_X value of octahedron BX_6 is ranging from 0.414 to 0.732 [30], the values of octahedron for all 30 cubic perovskites are in this range. However, octahedral factor (r_B/r_O value is not less 0.414) also is a necessary but not a sufficient condition for the formation of the cubic perovskite structure. The 91 systems in the range (r_B/r_O is not less 0.414) cannot form cubic perovskite structure as seen in Table **1**. According to Galasso's report [1], $LaVO_3$ which belong to $A^{3+}B^{3+}O_3$ perovskites, have cubic perovskite

Table 1. The Values of Ionic Radius, Tolerance Factor, Octahedral Factor and Formability of 173 Perovskite Solids

No.	Solids	r_A(Å) [5, 21]	r_B(Å) [5, 21]	Tolerance (t)	r_B/r_X	Formability*
1	$CsIO_3$	1.88	0.95	0.993	0.704	F
2	$CsNbO_3$	1.88	0.64	1.148	0.474	NF
3	$CsVO_3$	1.88	0.54	1.028	0.341	NF
4	KUO_3	1.64	0.76	1.002	0.563	F
5	$KPaO_3$	1.64	0.78	0.993	0.578	F
6	$KTaO_3$	1.64	0.64	1.062	0.474	NF
7	$KNbO_3$	1.64	0.64	1.062	0.474	NF
8	$KAsO_3$	1.64	0.46	1.168	0.341	NF
9	KVO_3	1.64	0.54	1.119	0.400	NF
10	KPO_3	1.64	0.38	1.222	0.281	NF
11	$KSbO_3$	1.64	0.60	1.084	0.444	NF
12	KIO_3	1.64	0.95	0.919	0.704	F
13	$KBiO_3$	1.64	0.76	1.002	0.563	NF
14	$NaTaO_3$	1.39	0.64	0.974	0.474	NF
15	$NaAlO_3$	1.39	0.535	1.028	0.396	NF
16	$NaWO_3$	1.39	0.62	0.983	0.459	NF
17	$NaAsO_3$	1.39	0.46	1.067	0.341	NF
18	$NaSbO_3$	1.39	0.60	0.994	0.444	NF
19	$NaPO_3$	1.39	0.38	1.120	0.281	NF
20	$NaBiO_3$	1.39	0.76	0.918	0.563	NF
21	$NaNbO_3$	1.39	0.64	0.974	0.474	NF
22	$NaUO_3$	1.39	0.76	0.918	0.563	NF
23	$NaVO_3$	1.39	0.54	1.025	0.341	NF
24	$LiNbO_3$	1.61	0.64	1.052	0.474	NF
25	$LiTaO_3$	1.61	0.64	1.052	0.474	NF
26	$LiVO_3$	1.61	0.54	1.107	0.400	NF
27	$LiAsO_3$	1.61	0.46	1.156	0.341	NF
28	$LiPO_3$	1.61	0.38	1.210	0.281	NF
29	$LiSbO_3$	1.61	0.60	1.073	0.444	NF
30	$LiBiO_3$	1.61	0.76	0.992	0.563	NF
31	$RbPaO_3$	1.72	0.78	1.019	0.578	F
32	$RbNbO_3$	1.72	0.64	1.091	0.474	NF
33	$RbTaO_3$	1.72	0.64	1.091	0.474	NF
34	$RbIO_3$	1.72	0.95	0.994	0.704	F
35	$RbUO_3$	1.72	0.76	1.029	0.563	F
36	$CuPO_3$	0.77	0.38	0.867	0.281	NF
37	$TiSbO_3$	0.67	0.60	0.732	0.444	NF
38	$AgBiO_3$	1.48	0.76	0.948	0.563	NF
39	$AgVO_3$	1.48	0.54	1.059	0.341	NF
40	$AgTaO_3$	1.48	0.64	1.006	0.474	NF
41	$AgNbO_3$	1.48	0.64	1.006	0.474	NF

(Table 1) contd…..

No.	Solids	r_A(Å) [5, 21]	r_B(Å) [5, 21]	Tolerance (t)	r_B/r_X	Formability*
42	$AgSbO_3$	1.48	0.60	1.026	0.444	NF
43	$TlIO_3$	1.70	0.95	1.084	0.704	NF
44	$BaFeO_3$	1.61	0.585	1.082	0.433	NF
45	$BaMoO_3$	1.61	0.65	1.047	0.481	F
46	$BaNbO_3$	1.61	0.68	1.031	0.504	F
47	$BaSnO_3$	1.61	0.69	1.026	0.511	F
48	$BaHfO_3$	1.61	0.71	1.016	0.526	F
49	$BaZrO_3$	1.61	0.72	1.011	0.533	F
50	$BaIrO_3$	1.61	0.625	1.060	0.463	NF
51	$BaPbO_3$	1.61	0.775	0.985	0.574	F
52	$BaTbO_3$	1.61	0.76	0.992	0.563	F
53	$BaPrO_3$	1.61	0.85	0.951	0.630	F
54	$BaCeO_3$	1.61	0.87	0.943	0.644	F
55	$BaAmO_3$	1.61	0.85	0.951	0.630	F
56	$BaNpO_3$	1.61	0.87	0.943	0.644	F
57	$BaUO_3$	1.61	0.89	0.934	0.659	NF
58	$BaPaO_3$	1.61	0.90	0.930	0.667	F
59	$BaThO_3$	1.61	0.94	0.914	0.696	F
60	$BaTiO_3$	1.61	0.605	1.071	0.448	NF
61	$BaGeO_3$	1.61	0.530	1.113	0.393	NF
62	$BaSiO_3$	1.61	0.40	1.196	0.296	NF
63	$BaMnO_3$	1.61	0.53	1.113	0.393	NF
64	$SrMnO_3$	1.44	0.53	1.049	0.393	NF
65	$SrVO_3$	1.44	0.58	1.022	0.430	NF
66	$SrFeO_3$	1.44	0.585	1.020	0.433	F
67	$SrTiO_3$	1.44	0.605	1.009	0.448	F
68	$SrTcO_3$	1.44	0.645	0.989	0.478	NF
69	$SrMoO_3$	1.44	0.65	0.986	0.481	F
70	$SrNbO_3$	1.44	0.68	0.972	0.504	F
71	$SrSnO_3$	1.44	0.69	0.967	0.511	F
72	$SrHfO_3$	1.44	0.71	0.958	0.526	F
73	$SrTbO_3$	1.44	0.76	0.935	0.563	NF
74	$SrAmO_3$	1.44	0.85	0.897	0.630	NF
75	$SrPuO_3$	1.44	0.86	0.893	0.637	NF
76	$SrCoO_3$	1.44	0.53	1.049	0.393	NF
77	$SrZrO_3$	1.44	0.72	0.939	0.533	F
78	$SrRuO_3$	1.44	0.68[a]	0.972	0.504	F
79	$SrSiO_3$	1.44	0.40	1.127	0.296	NF
80	$SrGeO_3$	1.44	0.53	1.049	0.393	NF
81	$SrMnO_3$	1.44	0.53	1.049	0.393	NF
82	$SrCeO_3$	1.44	0.87	0.889	0.644	NF
83	$SrPbO_3$	1.44	0.775	0.928	0.574	NF

(Table 1) contd…..

No.	Solids	r_A(Å) [5, 21]	r_B(Å) [5, 21]	Tolerance (t)	r_B/r_X	Formability*
84	$CaVO_3$	1.34	0.58	0.986	0.430	NF
85	$CaSiO_3$	1.34	0.40	1.087	0.296	NF
86	$CaGeO_3$	1.34	0.53	1.012	0.393	NF
87	$CaSnO_3$	1.34	0.69	0.932	0.511	NF
88	$CaUO_3$	1.34	0.89	0.849	0.659	NF
89	$CaZrO_3$	1.34	0.72	0.919	0.533	NF
90	$CaPbO_3$	1.34	0.775	0.895	0.574	NF
91	$CaMnO_3$	1.34	0.53	1.012	0.393	NF
92	$CaTiO_3$	1.34	0.605	0.973	0.448	NF
93	$CaCoO_3$	1.34	0.87	0.857	0.644	F
94	$CoTiO_3$	0.745	0.605	0.900	0.448	NF
95	$CoSiO_3$	0.745	0.40	0.847	0.296	NF
96	$CoMnO_3$	0.745	0.53	0.788	0.393	NF
97	$MgGeO_3$	0.72	0.53	0.867	0.393	NF
98	$MgTiO_3$	0.72	0.605	0.892	0.448	NF
99	$MgSnO_3$	0.72	0.69	0.718	0.511	NF
100	$MgSiO_3$	0.72	0.40	0.836	0.296	NF
101	$MnTiO_3$	0.83	0.605	0.928	0.448	NF
102	$MnGeO_3$	0.83	0.53	0.820	0.393	NF
103	$ZnTiO_3$	0.74	0.605	0.898	0.448	NF
104	$ZnSiO_3$	0.74	0.40	0.830	0.296	NF
105	$FeTiO_3$	0.78	0.605	0.912	0.448	NF
106	$FeSiO_3$	0.78	0.40	0.843	0.296	NF
107	$PbSiO_3$	1.19	0.40	1.026	0.296	NF
108	$PbGeO_3$	1.19	0.53	0.955	0.393	NF
109	$PbCeO_3$	1.19	0.87	0.809	0.644	NF
110	$PbTiO_3$	1.19	0.605	0.919	0.448	NF
111	$PbZrO_3$	1.19	0.72	0.868	0.533	NF
112	$CdGeO_3$	0.95	0.53	0.865	0.393	NF
113	$EuTiO_3$	1.23	0.670	0.903	0.496	NF
114	$EuAlO_3$	1.23	0.535	0.968	0.396	NF
115	$EuCrO_3$	1.23	0.615	0.928	0.456	NF
116	$EuFeO_3$	1.23	0.645	0.914	0.478	NF
117	$EuGaO_3$	1.23	0.620	0.926	0.459	NF
118	$EuBO_3$	1.23	0.230	1.155	0.170	NF
119	$CeAlO_3$	1.34	0.535	1.009	0.396	NF
120	$CeVO_3$	1.34	0.640	0.956	0.474	NF
121	$CeCrO_3$	1.34	0.615	0.968	0.456	NF
122	$GdAlO_3$	1.22	0.535	0.964	0.396	NF
123	$GdCrO_3$	1.22	0.615	0.925	0.456	NF
124	$GdFeO_3$	1.22	0.645	0.911	0.478	NF
125	$GdYO_3$	1.22	1.200	0.713	0.889	NF

(Table 1) contd…..

No.	Solids	r_A(Å) [5, 21]	r_B(Å) [5, 21]	Tolerance (t)	r_B/r_X	Formability*
126	$GdGaO_3$	1.22	0.620	0.922	0.459	NF
127	$GdTiO_3$	1.22	0.670	0.900	0.496	NF
128	$GdBO_3$	1.22	0.230	1.150	0.170	NF
129	$LaAlO_3$	1.36	0.535	1.017	0.396	NF
130	$LaCrO_3$	1.36	0.615	0.975	0.456	NF
131	$LaFeO_3$	1.36	0.645	0.961	0.478	NF
132	$LaGaO_3$	1.36	0.620	0.973	0.459	NF
133	$LaRhO_3$	1.36	0.665	0.951	0.493	NF
134	$LaTiO_3$	1.36	0.670	0.949	0.496	NF
135	$LaVO_3$	1.36	0.640	0.963	0.474	NF
136	$LaMnO_3$	1.36	0.645	0.961	0.478	NF
137	$LaCoO_3$	1.36	0.545	1.011	0.404	NF
138	$LaBO_3$	1.36	0.230	1.213	0.170	NF
139	$NdAlO_3$	1.27	0.535	0.983	0.396	NF
140	$NdCoO_3$	1.27	0.545	0.978	0.404	NF
141	$NdCrO_3$	1.27	0.615	0.943	0.456	NF
142	$NdFeO_3$	1.27	0.645	0.929	0.478	NF
143	$NdMnO_3$	1.27	0.645	0.929	0.478	NF
144	$NdTiO_3$	1.27	0.670	1.091	0.496	NF
145	$NdVO_3$	1.27	0.640	1.166	0.474	NF
146	$NdGaO_3$	1.27	0.620	0.940	0.459	NF
147	$PrAlO_3$	1.30	0.535	0.994	0.396	NF
148	$PrCrO_3$	1.30	0.615	0.954	0.456	NF
149	$PrFeO_3$	1.30	0.645	0.939	0.478	NF
150	$PrGaO_3$	1.30	0.620	0.951	0.459	NF
151	$PrMnO_3$	1.30	0.645	0.939	0.478	NF
152	$PrVO_3$	1.30	0.640	0.942	0.474	NF
153	$SmAlO_3$	1.24	0.535	0.972	0.396	NF
154	$SmCoO_3$	1.24	0.545	0.966	0.404	NF
155	$SmVO_3$	1.24	0.640	0.920	0.474	NF
156	$SmFeO_3$	1.24	0.645	0.918	0.478	NF
157	$SmYO_3$	1.24	1.200	0.718	0.889	NF
158	$SmCeO_3$	1.24	1.34	0.681	0.993	NF
159	$SmTiO_3$	1.24	0.670	0.907	0.496	NF
160	$SmBO_3$	1.24	0.230	1.159	0.170	NF
161	$YAlO_3$	1.20	0.535	0.957	0.396	NF
162	$YCrO_3$	1.20	0.615	0.918	0.456	NF
163	$YFeO_3$	1.20	0.645	0.904	0.478	NF
164	$YTiO_3$	1.20	0.670	0.893	0.496	NF
165	YBO_3	1.20	0.230	1.141	0.170	NF
166	$VCrO_3$	0.64	0.65	0.716	0.456	NF
167	$VAlO_3$	0.64	0.535	0.746	0.396	NF

(Table 1) contd…..

No.	Solids	r_A(Å) [5, 21]	r_B(Å) [5, 21]	Tolerance (t)	r_B/r_X	Formability*
168	$BiAlO_3$	1.03	0.535	0.893	0.396	NF
169	$BiGaO_3$	1.03	0.620	0.854	0.459	NF
170	$BiInO_3$	1.03	0.800	0.783	0.593	NF
171	$BiSmO_3$	1.03	1.24	0.650	0.919	NF
172	$BiFeO_3$	1.03	0.645	0.844	0.478	NF
173	$BiScO_3$	1.03	0.745	0.803	0.552	NF

*F represents that binary oxide systems can form cubic perovskite,
*NF represents that binary oxide systems can not form cubic perovskite,

structure previously, however, the later reports indicate that $LaVO_3$ and Medarde [31, 32], rare earth perovskite oxides, have orthorhombic structure [3, 34]. We have also found in Fig. (**5**) that the $A^{3+}B^{3+}O_3$ system does not show ''cubic perovskites'' region. Our results are good agreement with Medarde [31, 32], and may imply other criterion for cubic perovskites formability. In the Fig. (**5**), it can be seen that some systems of all 173 ''non-cubic perovskites'', including $SrPbO_3$, $SrTbO_3$, $SrTcO_3$, $AgBiO_3$, $AgNbO_3$ and $BaUO_3$ are wrongly classified in ''cubic perovskites'' region by the criterion mentioned above. However some points near the boundary between ''cubic perovskites'' and ''non-cubic perovskites'', as seen in Fig. (**5**), few points, representing like as $AgNbO_3$ (at 610°C) and $AgBiO_3$ just inside the boundary, which has distorted perovskite structure can transfer to cubic perovskite structure at 610°C [35].

CONCLUSION

We come to the conclusion that our model gives a simple and effective prediction criterion for cubic perovskites formability. New cubic perovskite structure compounds can be predicted by using this model, and their lattice constant can be predicted by a proposed relation of lattice constant in cubic perovskites, which was obtained in our previous study [21]. Using these models, we can seek for new cubic perovskites which lattice constant is close to compound semiconductor. Using these samples, regularities of formability of cubic perovskites are investigated by two empirical two-dimension structural map, One map is drawn by the ionic radii of cation A and B, another is spanned by octahedral factor (r_B/r_O) and the tolerance factor.

Through this study, the following conclusions are obtained:

1. In the R_A-R_B structural map (Figs. **2-4**), the systems with perovskite and those non perovskite are distributed in distinctively different regions, there exists a clear boundary between these two kinds of samples.
2. Octahedral factor is as important as the tolerance factor for cubic perovskites formability.
3. Both tolerance factor and octahedral factor are a necessary but not sufficient condition for cubic perovskites formability. Using these two factors, the cubic perovskites formability can be reliably predicted.
4. In the structural map (Fig. **5**) that is drawn by the tolerance factor and octahedral factor the points for cubic perovskites and those for non-cubic perovskites are located in different zones *via* clear boundary defined by Eqs. (2)–(5). These equations form the criteria for cubic perovskites formability.

The simple method presented in this work will be helpful to material scientists for finding new substrate or buffer materials in compound semiconductor epitaxy.

REFERENCES

[1] Galasso F. Perovskites and High-Tc Superconductors. Gordon and Breach Science Pub: London 1990.
[2] Iwahara H, Balkanski M, Takahashi M, Tuller HL, Eds. Solid State Ionics. Elsevier: Amsterdam 1992.
[3] Mori T, Aoki K, Kamegashira N, Shishido T. Crystal structure of $DyMnO_3$. Mater Lett 2000; 42: 387-9.
[4] Terki R, Feraoun H, Bertrand G, Aourag H. Full potential calculation of structural, elastic and electronic properties of $BaZrO_3$ and $SrZrO_3$. Phys Stat Sol (b) 2005; 242(5): 1054-62.
[5] Chonghe L, Kitty Chi Kwan Soh, Ping W. Formability of ABO_3 perovskites. J Alloys Comp 2004; 372: 40-48.
[6] Cabuk S, Akkus H, Mamedov AM. Electronic and optical properties of $KTaO_3$ Ab initio calculation. Physica B 2007; 394: 81-5.
[7] Wang H, Wang B, Wang R, Li Q. Ab initio study of structural and electronic properties of $BiAlO_3$ and $BiGaO_3$. Physica B 2007; 390: 96-100.
[8] Moreira RL, Dias A. Comment on prediction of lattice constants in cubic perovskites. J Phys Chem Solids 2007; 68: 1617-22.
[9] Jiang LQ, Guo JK, Liu HB, *et al*. Prediction of lattice constant in cubic perovskites. J Phys Chem Solids 2006; 67: 1531-6.
[10] Ramesh R, Spaklin NA. Multiferroics: progress and prospects in thin films. Nat Mater 2007; 6: 21-9.
[11] Scott JF. Nanoferroelectrics: statics and dynamics. J Phys Cond Matt 2006; 18: R361-86.
[12] Bokov AA, Ye ZG. Recent progress in relaxor ferroelectrics with perovskite structure. J Mater Sci 2006; 41: 31-52.
[13] Ormerod RM. Solid oxide fuel cells. Chem Sov Rev 2003; 32: 17-28.
[14] Li C, Wang B, Wang R, Wang H, Lu X. First-principles study of structural, elastic, electronic, and optical properties of hexagonal $BiAlO_3$. Physica B 2008; 403: 539-43.
[15] Huang YH, Dass RI, Xing ZL, Goodenough JB. Double Perovskites as Anode Materials for Solid-Oxide Fuel Cells. Science 2006; 312: 254-7.
[16] Gupta A, Hussey BW, Shaw TM. Epitaxial growth of thin films of $SrTi_{1-x}Ru_xO_{3-\delta}$ by pulsed laser deposition. Mater Res Bull 1996; 31: 1463-70.
[17] Takahashi H, Ohta J, Fujioka H, Oshima M. Growth of GaN on $NdGaO_3$ substrates by pulsed laser deposition. Thin Solid Films 2002; 407: 114-17.
[18] Shimamura V, Tabata H, Takeda H, Kochurikhin VV, Fukuda T. Growth and characterization of $(La,Sr)(Al,Ta)O_3$ single crystals as substrates for GaN epitaxial growth. J Cryst Growth 1998; 194: 209-13.

[19] Ito M, Shimamura K, Pawlak DA, Fukuda T. Growth of perovskite-type oxides (RE, Sr)(Al, Ta)O_3 as substrates for GaN epitaxial growth (RE=La, Nd). J Cryst Growth 2002; 235: 277-82.

[20] Eisenbeiser K, Emrickm R, Droopad R, *et al*. GaAs MESFETs fabricated on Si substrates using a $SrTiO_3$ buffer layer. IEEE Electron Devices Lett 2002; 23: 300-2.

[21] Verma AS, Kumar A, Bhardwaj SR. Correlation between ionic charge and the lattice constant of cubic perovskite solids. Phys Stat Sol (b) 2008; 245: 1520-6.

[22] Mooser E, Pearson WB. On the crystal chemistry of normal valence compounds. Acta Cryst 1959; 12: 1015-22.

[23] Muller O, Roy R. The Major Ternary Structural Families. Springer New York 1974.

[24] Bhalla AS, Guo RY, Roy R. The perovskite structure – a review of its role in ceramic science and technology. Mater Res Innov 2000; 4: 3.

[25] Sondena R, Stolen S, Ravindran P, Grande T, Allan NL. Corner- versus face-sharing octahedra in *A*MnO_3 perovskites (*A*=Ca, Sr, and Ba). Phys Rev B 2007; 75: 184105-15.

[26] Fava FF, Arco PD, Orlando R, Dovesi R. A quantum mechanical investigation of the electronic and magnetic properties of $CaMnO_3$ perovskite. J Phys Cond Matt 1997; 9: 489-98.

[27] Syono Y, Akimoto S I, Kohn K. Structure Relations of Hexagonal Perovskite-Like Compounds ABX_3 at High Pressure. J Phys Soc Jpn 1969; 26: 993-9.

[28] Mitchell RH. Perovskites Modern and Ancient. Almaz Press: Thunder Bay Canada 2002.

[29] Sondena R, Ravindran P, Stolen S, Grande T, Hanfland M. Electronic structure and magnetic properties of cubic and hexagonal $SrMnO_3$. Phys Rev B 2006; 74: 144102-14.

[30] Wang ZL, Kang ZC. Functional and Smart Materials Structural Evolution and Structure Analysis. Plenum Press: New York 1998.

[31] Medarde ML. Structural, magnetic and electronic properties of $RNiO_3$ perovskites (R = rare earth). J Phys Cond Matt 1997; 9: 1679-1707.

[32] Zhou JS, Yan HQ, Goodenough JB. Bulk modulus anomaly in *R*CoO_3 (*R*=La, Pr, and Nd). Phys Rev B 2005; 71: 220103(R)-7(R).

[33] Shannon RD. Revised effective ionic radii and systematic studies of interatomic distances in halides and chalcogenides. Acta Crystallogr 1976; A32: 751-76.

[34] Khan R T A, Bashir J, Iqbal N, Khan M N. Crystal structure of $LaVO_3$ by Rietveld refinement method. Mater Lett 2004; 58: 1737-40.

[35] Ali R, Yashima M. Space group and crystal structure of the Perovskite $CaTiO_3$ from 296 to 1720 K. J Solid State Chem 2005; 178: 2867-72.

Received: August 5, 2008 Revised: September 28, 2008 Accepted: October 8, 2008